Montmorillonite nanoclay based formulation for controlled and selective release of volatile essential oil compounds

Kamal Essifi*[a], Abdourahim Hammani[b], Doha Berraaouan[a], Ali El Bachiri[a], Marie-Laure Fauconnier[c], and Abdesselam Tahani*[a]

[a]Physical Chemistry of Natural Substances and Process Team, Laboratory of Applied Chemistry and Environment (LCAE-CPSUNAP), Department of Chemistry, Faculty of Sciences, University Mohamed Premier, Oujda, Morocco.

[b]IUT Creteil-Vitry, Department of Chemistry, University of Paris-Est Creteil Val de Marne (UPEC), France.

[c]Laboratory of Chemistry of natural molecules, Gembloux Agro-Bio Tech, University of Liège, Belgium.

**Corresponding authors: E-mail: kamal.essifi.lpapc@gmail.com / a1.tahani@ump.ac.ma*

Abstract

In the current study, a green method that can be easily used in different industrial applications, based on the modification of sodium exchanged montmorillonite (Na^+-Mt) with essential oils (EO) such as thyme oil, thymol and carvacrol was presented. The obtained results show the prepared clays-essential oils hybrids were promising nanomaterials to encapsulate the active compounds and to control their release selectively in the functional applications. X-ray diffraction (XRD) analysis was used to study the adsorption of EO, thymol and carvacrol molecules, in the interlayer space. To verify the adsorption of thyme EO, thymol and carvacrol into Na^+-Mt layers and to determine the temperature range where the EO, thymol and carvacrol release took place, thermogravimetric analysis (TG) was used. Attenuated total reflecting-Fourier-transform infrared (ATR-FTIR) spectroscopy was used to verify and to study the adsorption mechanism. The obtained results show that the interlayer space of Na^+-Mt was not affected by the adsorption of thyme EO, thymol or carvacrol molecules. The release of the adsorbed molecules of thyme EO, thymol or carvacrol from Na^+-Mt surface was obtained above 180°C. Combination of simulation with all obtained experimental results, confirm that the adsorption process of thyme EO, thymol, and carvacrol molecules on the Na^+-Mt took place on the external surface i) by hydrogen bonds between the OH groups of thyme EO, thymol or carvacrol molecules and OH groups of Na^+-Mt surface, and ii) by hydrogen bonds between these adsorbed molecules. The release study shows that the adsorption of EO like thyme, and

its constituents such as thymol and carvacrol onto an inorganic porous material such as Na^+-Mt provides extended controlled release of all adsorbed active molecules with their chemical stability due to the protection against environmental conditions. In addition, the release of thyme oil constituents (like thymol and carvacrol) occurs by a selective process in time.

Keywords: Na^+-montmorillonite; Thyme oil; Thymol; Carvacrol; Controlled release

1. Introduction

Essential oils (EO) are natural, volatile liquids extracted from various plants which are responsible for several use in medicine, agriculture, and perfumes for many years [1]. Interest in these EO has massively increased in recent years, thanks to their physico-chemical and biological properties. Actually, numerous authors have shown biocide, antioxidant and antimicrobial activities, which are usable in many areas [2–4]. EO are essentially composed of simple molecules called terpenes and can be easily extracted using a variety of different distillation and extraction techniques [5].

Recently, the use of EO as biopesticides has become alternative methods to control various types of insects such as the treatment of honeybee pests (*Apismellifera L.*) as a Varroa destructor [6–10] Beekeepers in Morocco have been found that the Varroa has fewer impact on colonies of bees foraging on thyme stands (*Thymus satureioides*) [10]. They are also using the plant directly for fumigating the beehives to control the pest.

Thymus satureioides Coss. and *Origanum elongatum* Bonn. formations exist wildly in the central and western High Atlas and in north-eastern Rif regions of Morocco, respectively [10,11]. So, they are important natural sources of EO. Thyme EO contains a number of active compounds such as thymol, carvacrol, p-cymene, myrcene, linalool, borneol, and others [12], although most of them are showing important antioxidant and antimicrobial effects against a wide variety of gram-negative or gram-positive bacteria. The phenols such as thymol, rosmarinic acid, and carvacrol are the most important active compounds of thyme EO [13,14]. The carvacrol is a high concentration monoterpenoid compound contained in oregano EO extracted from the origanum and thyme plants show a high acaricidal potential [10,15–20]. In addition, many important biological properties, such as antioxidant antimicrobial, anti-mutagenic, antitumor, cell-protective, and anti-inflammatory activities, have been reported for thyme EO, thymol, and carvacrol [10,17,20–22]. EO bioactivity is primarily attributed to its

chemical structure, and in specific to the functional groups of the principal constituents [10,23,24].

However, their direct use may be limited by their aromatic properties and their instability to the environmental conditions. In addition, to prevent infection from living with resistant parasites, a sequential and controller release of EO compounds is necessary. Therefore, the adsorption and the encapsulation may be a useful strategy to be further studied and widen the application of thymol and thymol-based ingredients such as thyme oil [25,26].

Recently, adsorption of EO onto a nonporous inorganic material has been suggested to control the release and protection from polymer processing condition [27–33]. Thanks to its layered structure and high surface area as well as its high cation exchange capacity and its ability to swell, the montmorillonite (Mt) is an ideal adsorbent and nano-carrier of such EO [27–30,33–36]. In previous studies [27,29–33], the adsorption of EO on inorganic nanomaterials was obtained using various organic solvents, such as acetone [31–33] or heptane [30]. Indeed, possible residues of solvents in the final materials tend to have been a disadvantage of using such modified clay minerals in the functional applications.

Moreover, in the study reported by Giannakas et al., (2017), a method for the adsorption of EO on clays was carried out via adsorption/evaporation with using the high temperature. The sensitivity of EO to temperature introduces the possibility to endanger their physical-chemical and biological properties. Recently, an adsorption method was documented for use with only essential oil components such as allyl isothiocyanate, carvacrol, transcinnamaldehyde, diallyl disulphide, eugenol, and thymol [37]. This method based on the direct mixing of montmorillonite samples and essential oil components followed by a heating step. In this work, a green evaporation/adsorption method for the adsorption of essential oils and EO components on clay minerals is presented without the use of organic solvents and without using the high temperature.

The aim of the preparation approach was to produce powdered final EO-clay mineral hybrids in order to make their usage easier to control the release of active compounds of EO which are well-known for their significant acaricidal, fungicidal, larvicidal, and insecticidal properties [6–10]. The EO that were used were thyme oil, thymol and carvacrol. XRD, TG and FTIR characterization methods were employed to investigate the mechanism and the effect of adsorption of thyme oil, thymol and carvacrol into a natural sodium exchanged hydrophilic

montmorillonite (Na^+-Mt), and the GC analysis was used to study the release in gas phase of all EO from obtained Na^+-Mt/EO hybrids.

2. Materials and Methods

2. 1. Essential oil and active compounds used

Thyme EO from Jerada (Province of Oriental region Morocco) was extracted by steam distillation, Thymol (2-isopropyl-5-methylphenol, 99% purity) and Carvacrol (5-isopropyl-2-methylphenol, CARV, 98% purity) were purchased from Sigma—Aldrich. A result of GC-MS analysis of different adsorbents, such as thyme EO, thymol, and carvacrol was presented in (4.6 section).

2. 2. Purification and preparation of sodium exchanged montmorillonite

The starting raw clay from Nador (North-East of Morocco) is an industrial bentonite rich in montmorillonite [38]. The montmorillonite used in this study was purified according the method already described in a previous paper [38]. Briefly, pretreatment of the raw bentonite is carried out by a series of washing with distilled water to make the elimination of the impurities of all the crystalline phases (such as quartz, calcite, feldspar…) and to obtain a well-defined granular fraction with size ≤ 2 µm. This granular fraction has been followed by a series of treatments by sodium chloride solution to prepare the sodium montmorillonite homo-ionized (sodium exchanged montmorillonite). In practice, this purification consists of dispersing a mass of 1 kg of crude clay in 5 liters of distilled water with a solid/liquid ratio: 1:5. The mixture was mechanically stirred for an hour till the complete homogenization. Then a treatment with HCl (0.5 M) was made to remove carbonate. To oxidize organic matter a washing with H_2O_2 (10%) of the resulting mixture was made. A number extensively (6 times) of washing with NaCl 1 M followed by centrifugation of the resulting product was made to give saturated clay minerals. The fraction enriched in impurities (the dark gray residue in the centrifuge tube) was eliminated. The clear fraction was then washed and dialyzed with distilled water until the conductivity in the dialysis bath was less than 2 µS/cm (conductivity of used distilled water). The obtained dispersion was then air-dried and was gently grounded to obtain powder sodium exchanged montmorillonite (Na^+-Mt), and the necessary characterizations have been made.

The surface areas and the pores volume of the samples were determined by Micrometrics ASAP 2000 volumetric adsorption-desorption apparatus, using nitrogen as adsorbent [39], the

result gives specific surface S_{BET} = 83.49m^2g^{-1}, total pore volume V_t = 0.213 cm^3g^{-1}, specific external surface S_{ext} = 82.93m^2g^{-1}.

The cation exchange capacity (CEC) was also determined by adsorption of a copper ethylene diamine complex [40,41], the obtained CEC is 90 meq/100 g clay mineral. Chemical analyses of the samples are given in Table 1.

Table 1. Chemical composition (wt. %) of sodium modified and raw montmorillonite.

	SiO_2	Al_2O_3	CaO	MgO	Fe_2O_3	Na_2O_2	K_2O	SO_3	$CuOTiO_2$		ZnO
Na^+-Mt	61.17	15.13	4.00	6.00	3.25	1.1	0.52	0.38	0.13	0.12	0.1
Raw-Mt	64.05	16.33	4.13	6.69	3.44	1.12	0.65	0.37	0.09	0.1	0.05

2. 3. Preparation of Na^+-Mt/Thyme oil, Na^+-Mt/Thymol and Na^+-Mt/Carvacrol hybrids

Loading of thyme oil and its constituents thymol and carvacrol into Na^+-Mt was carried out via evaporation/adsorption procedure without using high temperatures and organic solvents. This innovative procedure of directly mixing EO with clay minerals, avoids the formation of clay/EO slurries. The heating of EO has not been done in order to not to endanger the physical-chemical and biological properties. Before the evaporation/adsorption procedure, the Na^+-Mt is dried in an oven at 120°C overnight. 1g of this sample was spread out in an aluminum beaker and placed in a desiccator under vacuum for more than 2 hours in the presence of separate containers, containing 250g of anhydrous $CaCl_2$ and 250g of P_2O_5 to remove all traces of moisture, the air gases in the desiccator and subsequently the water adsorbed in the surface of the clay (Figure 1a). Then, the anhydrous salts were replaced by 2g of EO, thymol or carvacrol, and the system is kept under vacuum for 1 to 2 hours (Figure 1b). The temperature inside the desiccator is 30 °C.

The clay mineral samples are left under an EO atmosphere, then weighed after variable equilibrium time in hours (see the day) to know the quantities of EO adsorbed and at the end let the system equilibrate under vacuum for a certain period (approximately 10 days). Under these conditions the most volatile EO components were evaporated and adsorbed into Na^+-Mt, when the evaporation-adsorption procedure ended the obtained Na^+-Mt/EO clay hybrids were labeled and put in sealed closed glass beakers for further characterization.

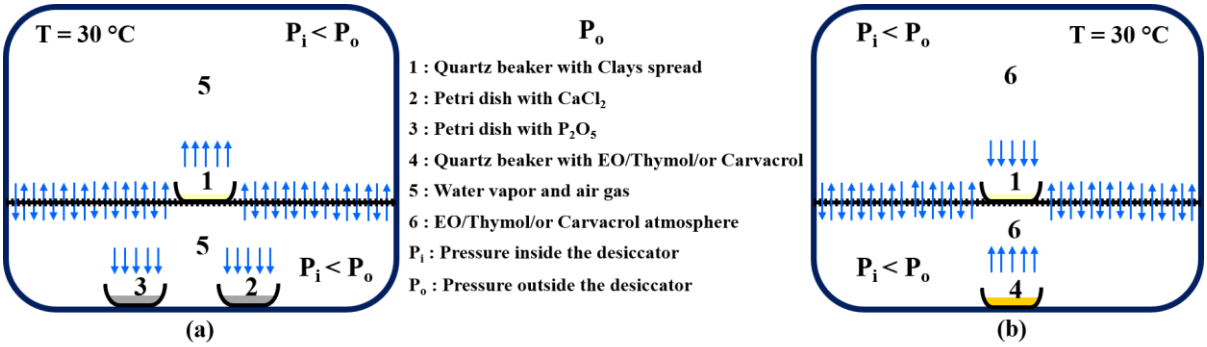

Fig. 1. Gas evacuation and desorption of adsorbed water in the clay surface (a), evaporation/adsorption process of thyme EO, thymol and carvacrol on Na^+-Mt (b).

3. Characterization techniques

3. 1. XRD analysis

XRD analysis was used to estimate the interlayer space of all clay mineral EO hybrid powders using a Shimadzu XRD-6000 X-ray diffractometer in the range from 2 to 40 (2θ) with a step size of 0.02° 2θ angle and CuKα radiation (λ = 1.5418 Å).

3. 2. TG analysis

TG experiments were realized with a Shimadzu DTG-60 apparatus. A sample mass of Na^+-Mt, Na^+-Mt/EO, Na^+-Mt/thymol, Na^+-Mt/carvacrol or of pure adsorbents was loaded in an alumina crucible and heated from room temperature to 900°C (heating rate: 5°C min^{-1}) in the air flow (75 mL min^{-1}).

3. 3. Attenuated total reflecting-Fourier-transform infrared (ATR-FTIR) investigation

The functional groups of EO on the Na^+-Mt surface were investigated by ATR-FTIR which was recorded on a Jasco4700-ATR spectrophotometer (Shimadzu, Japan). These experiments were also used to confirm the presence of EO in the Na^+-Mt nanoparticles. Powder of dried sample was sandwiched between the ATR accessory and the diamond crystal. Spectra of samples were recorded in the wavelength region between 400 and 4000 cm^{-1}. Each spectrum was obtained by averaging 32 scans at a resolution of $4cm^{-1}$. Spectra of substrates before and after adsorption of the thyme EO, thymol, and carvacrol were compared respectively to spectra of the pure thyme EO, thymol, and carvacrol in order to confirm the presence of these adsorbed molecules. The experiments were performed in triplicates and showed good reproducibility.

3. 4. Simulation details

The annealing simulation in the canonical ensemble (constant atom number, volume and energy [NVE]) was utilized to understand the mechanism of adsorption of thymol, and to determine the arrangement of thymol molecules on the external surface of Mt on the basis of minimum adsorption energy of thymol. The vacuum slab with 4a×3b×1c crystal unit was created and the vacuum slab was orientated along the c-plane with crystal thickness of 12.6Å. Adsorption locator was used to generate the models depicting thymol on the surface of Mt. All adsorption locator calculations were performed using compass force field with the surface region defined by atom set, and with the fixed number of 10 configurations. All simulations were executed using the adsorption locator and forcite Modules of Materials Studio (version 17.1.0.48). The force field used is COMPASS 2, the system was subjected to energy minimization for geometry optimization before anneal simulations were conducted. For minimization calculation maximum iterations of 50,000 was used with an ultra-fine convergence level. The anneal simulation using NVE lasted for $5 \cdot 10^{-12}$ seconds (ps) with a time step of 10^{-15} seconds (fs). The obtained results are presented in (4. 5 section).

3. 5. Essential oils release study

The release study of EO from hybrid materials nanoparticles was carried out in the gas phase, using a Hewlett Packard 6890 gas chromatography equipped with a Hewlett Packard 6890 mass selective detector and an BPX25 capillary column with 5% diphenyl, 95% dimethylpolysiloxane phase (30 m × 0.25 mm inner diameter × 0.25 µm film thickness), coupled to a QP2010 MS. Split is the injection mode. The pure helium gas (99.99%) was used as carrier gas with a constant flow rate of 3 mL/min. The injection, ion source, and interface temperatures were all set at 250°C. The temperature program used for the column oven was 5 °C (held for 1 min), heated to 250°C at 10°C/min and held for 1 min. The ionization energy was set at 70 eV. Finally, compounds were identified by comparison of their retention times with those of authentic standards and their mass spectrum fragmentation patterns with those found in databases or those stored on the National Institute of Standards and Technology (NIST) 147, 198 compounds. LabSolutions (version 2.5) was used for data collection and processing: i) to confirm the success of EO adsorption on the Mt; ii) to understand the affinity of EO with the Na^+-Mt nanoparticles; and iii) to determine the stability of EO for the controlled releasing from the Mt nanoparticles, which is important for further applications of EO-loaded inorganic clay nanoparticles.

4. Results and discussion

4. 1. Gas phase adsorption of essential oils

The adsorption kinetics in gas phase of EO of thyme, thymol and carvacrol on Na^+-Mt are represented in Figure 2. The results for the adsorption of thyme show that the adsorption kinetics are very rapid step to the first day, approximately 113mg of thyme/g of Mt was adsorbed (72%). After one day the adsorption kinetics are slow, in which the amount adsorbed increases periodically every two days until the fourth day when it reaches a maximum adsorption 160 mg of thyme/g of Mt.

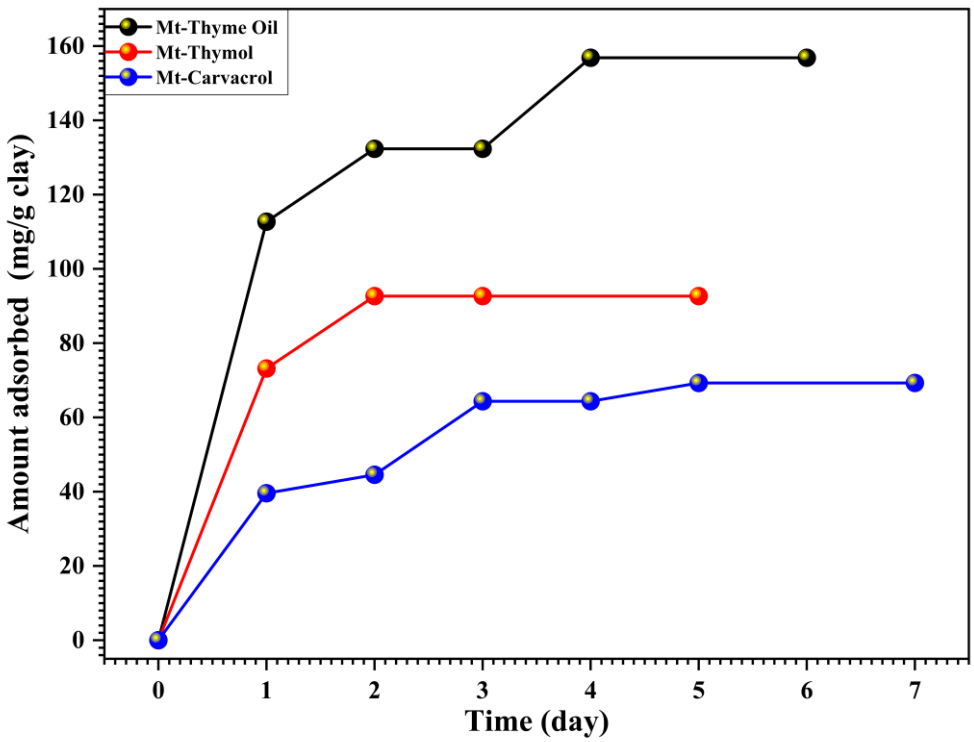

Fig. 2. Adsorption kinetics in gas phase of EO of thyme, thymol and carvacrol on Na^+-Mt.

The results show that the kinetics of thymol adsorption is rapid in the first two days, with approximately 93mg of thymol/g of Mt has been adsorbed (100%). After two days the kinetics of adsorption is constant. The carvacrol adsorption results show that the adsorption

kinetics is fast in the first three days, approximately 64mg of carvacrol/g of Mt is adsorbed (91%). After the first three days, the adsorption kinetics is slow as shown by the blue curve, in which the adsorbed amount increases until the fifth day and reaches a maximum adsorption of 70mg of carvacrol/g of Mt (100%).

According to the results of the gas phase adsorption of EO of thyme and its constituents, thymol and carvacrol, thyme EO is better absorbed than thymol and carvacrol on Na^+-Mt. In addition, thymol adsorbs better than carvacrol on the Na^+-Mt.

On the other hand, the maximum adsorption kinetics is faster in the case of thymol, it occurs from the second day whereas it occurs only around the fourth day for thyme oil and the maximum adsorption kinetics only comes on for the fifth day for carvacrol. These results allow to choose the adequate constituent for the encapsulation of the active material and to predict the adsorption time.

4. 2. XRD analysis

In Figure 3, are presented the XRD diffractograms of the obtained hybrid materials after EO, thymol, and carvacrol adsorption into Na^+-Mt and of purified Na^+-Mt (included for comparison). The d(001)-values for purified Na^+-Mt and all Na^+-Mt/EO, Na^+-Mt/thymol, and Na^+-Mt/carvacrol hybrids were calculated and reported in Table 2.

The examination of all XRD diffractograms (Figure 3), shows that the 001 reflection of all Na^+-Mt modified with the various adsorbents did not show a significant variation of 2 theta values in comparison to the purified Na^+-Mt. The d(001)-values for all the hybrid samples were almost the same as the d(001)-value of Na^+-Mt sample (Table 2).

Table 2. Amount adsorbed and d(001)-values, of Na^+-Mt, and the obtained hybrids Na^+-Mt/thyme oil, Na^+-Mt/thymol and Na^+-Mt/carvacrol.

	Amount adsorbed (mg EO/g Mt)	**d(001)(Å)**
Na^+-Mt	-	12.6
Mt-Thyme Oil	160	12.90
Mt-Thymol	93	12.84
Mt-Carvacrol	70	12.82

As the interlayer space between Na^+-Mt layers is not higher in the modified materials than in the purified Na^+-Mt, this suggests that the adsorption of the thyme EO, thymol and carvacrol

on Na^+-Mt mainly took place on the external surface of Na^+-Mt by adsorbent-adsorbate electrostatic interactions, similarly to the results reported by [26,30].

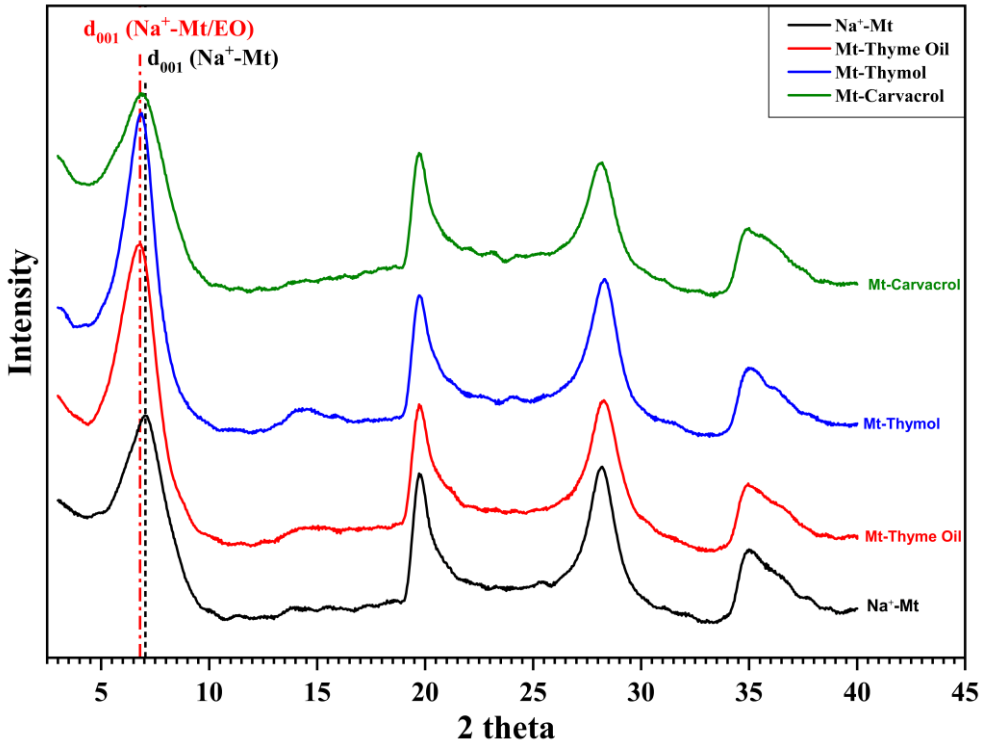

Fig. 3. XRD diffractograms for the six substrates between 2θ values of 2 and 45 °, highlighting the differences in d(001) reflections between the natural Na^+-Mt and the obtained Na^+-Mt/EO hybrids.

4. 3. TG experiments

The TG plots of and all obtained as well as Na^+-Mt purified are presented. The TG plots of pure essential thyme oil and EO constituents (thymol, carvacrol) (Figure 4a) show that all EO mass loss started above 100°C and ended before 220°C (dotted lines in Figure 4a). In all obtained Na^+-Mt/EO hybrids (dotted lines in Figure 4b) the mass loss started below 180°C and finished before 600°C where the dehydroxylation of Na^+-Mt has been initiated [42,43]. Two mass loss steps were observed in this total mass loss, the low-temperature step below 180°C and the high-temperature step above 180°C to approximately 600°C.

In agreement with X-ray results, where lower d-spacing was obtained for all obtained Na^+-Mt/EO, Na^+-Mt/thymol, and Na^+-Mt/carvacrol hybrids, the following conclusions can be obtained:

i) water molecules were not desorbed by applied vacuum in the first step of the adsorption process (see Figure 1a), so, they are being adsorbed in the Na^+-Mt interlayer space and were desorbed at the first mass loss step at the low temperature (below 180°C)

ii) EO, thymol, and carvacrol molecules were surely adsorbed on the external Na^+-Mt surface and were released during the second mass loss step at the higher temperatures (above 180°C). Similar results have been found by [26], suggesting that the oregano, thyme, and basil essential oils were probably adsorbed on the external Na^+-Mt surface through hydrogen bonds between OH groups of EO and OH groups of Na^+-Mt.

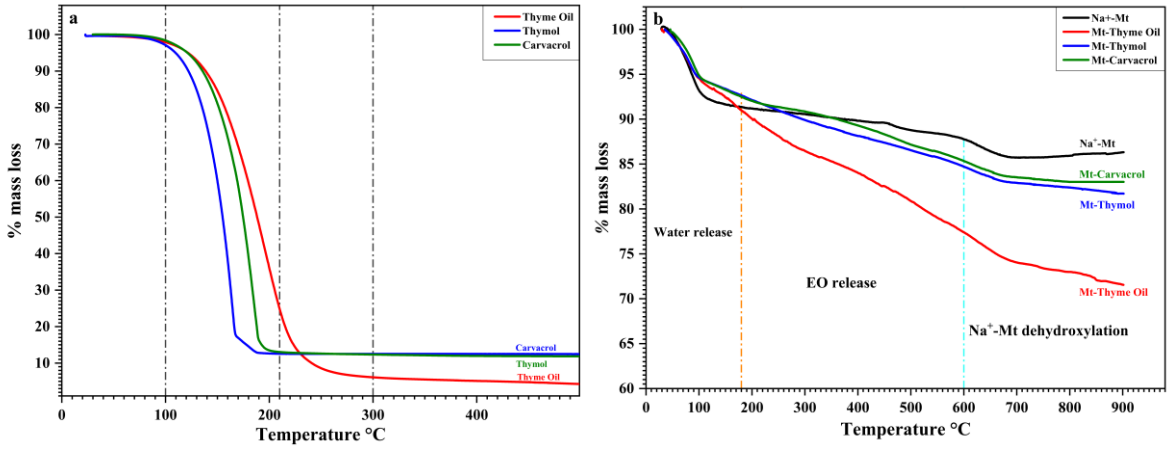

Fig. 4. TG curves of (a) thyme oil, thymol, carvacrol, and (b) purified Na^+-Mt and all obtained Na^+-Mt/EO hybrids.

The mass loss values during these two distinguished steps, as well as the total mass loss values, were calculated and presented in Table 3 for pure adsorbents such as thyme EO, thymol, and carvacrol and for all Na^+-Mt/thyme oil, Na^+-Mt/thymol, and Na^+-Mt/carvacrol hybrid materials. As can be seen: the EO are more thermally stable in hybrid form. This result corroborates the use of obtained Na^+-Mt/EO, Na^+-Mt/thymol, and Na^+-Mt/carvacrol nanostructured hybrids in controlled release functional applications where it will be expected to have different release rates with a selective release.

Table 3. Designation and % Mass loss values of thyme oil, thymol, carvacrol, purified Na^+-Mt and all obtained Na^+-Mt/EO hybrids calculated from TG curves.

Code name	% mass loss below 180°C	% mass loss above 180°C	Total % mass loss
Thyme Oil	85 (below 220°C)	11 (above 220°C)	96
Thymol	98 (below 220°C)	0	98
Carvacrol	98 (below 220°C)	0	98
Na^+-Mt	8.5	5.5	14
Mt-Thyme Oil	9	19.5	28.5
Mt-Thymol	7.5	11	18.5
Mt-Carvacrol	7.5	9.5	17

4. 4. ATR-FTIR measurements

The ATR-FTIR spectra of the adsorbents such as thyme oil, thymol, and carvacrol, and all obtained Na^+-Mt/thyme oil, Na^+-Mt/thymol, and Na^+-Mt/carvacrol hybrid materials were presented in Figure 5. A series of vibrations and elongation bands were classified as follows:

-For all adsorbents, the thyme oil, the thymol, and the carvacrol, abroad band at ~3400 cm^{-1} attributed to hydrogen-bonded O-H stretching is observed.

-Bands at ~3050-3000 cm^{-1} were assigned to the aromatic cycle and alkenic H-C=C-H stretch vibrations [26,30,44].

-In all the adsorbents spectra, three observed bands in the range 2850–3000 cm^{-1} (indicated with a dotted line in Figure 5) were assigned to the C-H stretching vibration of aliphatic CH_2 bonds. This group of bands was a strong indicator of adsorption of thyme oil, thymol, and carvacrol on Na^+-Mt, due to the absence of bands in this wavenumbers range in the pure Na^+-Mt spectrum.

- In wavenumbers range 1500 $cm^{-1}$and 1000 cm^{-1}several bands for all the adsorbents were observed, which were assigned to the C-O-H bending and the C-H bending of the aliphatic

groups (CH_2). Noteworthy, their overlap with those of the Na^+-Mt spectrum is not expected. Consequently, they should be visible in the spectra of the hybrid materials [26,30]. Finally, the observed bands below 1000 cm^{-1}were not considered as significant for adsorption study, due to their overlap with those of the Na^+-Mt spectrum [26,30].

In the ATR-FTIR Na^+-Mt spectrum (Figure 5), the following attributions are shown:

A band at ~3620 cm^{-1} was attributed to the characteristic absorption band of OH group stretching bonded with Al^{3+} cation [36,42,45]; a large band centered at ~3400 cm^{-1} assigned to the stretching vibration of the O-H bonds of the H_2O molecules; the observed band at ~1633 cm^{-1} was assigned to the bending vibrations of the O-H bonds of the H_2O molecules; the obtained bands at wavenumbers ~1110 $cm^{-1}$and at ~981 cm^{-1}(see Figure 5) were attributed to the stretching vibration of Si-O [38,42,46]. The observed bands at 913, 878, and 841 cm^{-1}represent the OH bending modes. Moreover, the bands at, ~913 cm^{-1}, ~878 $cm^{-1}$and ~841 cm^{-1} were respectively attributed to the bending mode of Al-Al-OH; Al-Fe-OH; and Fe-Fe-OH groups [38,42,47,48].

The ATR-FTIR spectra of Na^+-Mt with loadings of EO of thyme, thymol and carvacrol are presented also in Figure 5. In agreement with XRD and TG results of all obtained Na^+-Mt hybrids materials, the OH stretching modes at 3400 cm^{-1}support the suggestion that water molecules remain adsorbed in the interlayer spaces of Na^+-Mt after the applied vacuum. In all the obtained hybrid samples, it is clear that the suggested adsorption of thyme oil, thymol, and carvacrol molecules on the external Na^+-Mt surface has occurred, leading to the observed two groups of bands, in the range of 1200 to 1500 cm^{-1}(denoted with dotted rectangular in Figure 5) and 2800 to 3050 cm^{-1}(denoted with a dotted line in Figure 5d) which were characteristic EO, thymol and carvacrol molecules bands. To call attention, all these characteristic bands were denoted with different colors dot lines in Figure 5. In addition, for all obtained hybrid materials a shift of bands to higher wavenumbers was observed, accompanied by stretching bands in the case of the second group of bands at the 2800–3050 cm^{-1} range (see Figure 5d). Furthermore, in the higher wavenumbers part, was observed broadening bands of the characteristic Al-OH group at ~3620 cm^{-1} for all obtained hybrid Na^+-Mt (see Figure 5d).

After studying the relationship between the shift of aliphatic C-H bands to the higher wavenumbers in 3050-2800 cm^{-1} range and their broadening and the increasing stretching band of the characteristic Al-OH group of Na^+-Mt, it can be confirmed that the thyme EO, thymol, and carvacrol molecules were bonded on the external Na^+-Mt surface by hydrogen bonds

between EO, thymol or carvacrol OH groups and OH groups of Na^+-Mt surface. Hydrogen bonds between adsorbed molecules were also suggested. This proposed adsorption process shows a correlation between ATR-FTIR (strong interactions between OH groups of adsorbed molecules and OH groups of external Na^+-Mt surface), XRD (no significative increasing of Na^+-Mt interlayer spaces was observed, Figure 3) and TG results, see Table 3 (the EO, thymol, and carvacrol molecules released from Na^+-Mt above 180°C signifying a strong created hydrogen bonds).

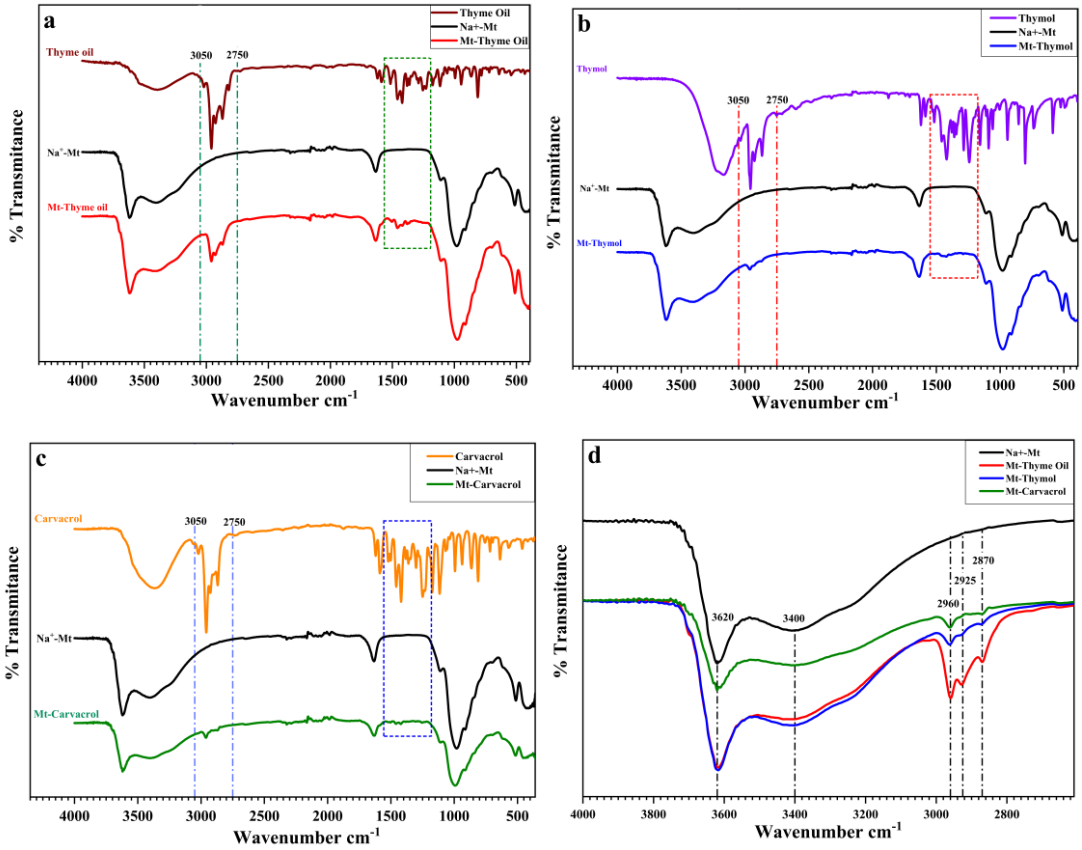

Fig. 5. Attenuated total reflecting-Fourier-transform infrared spectra (ATR-FTIR) of Na^+-Mt, thyme oil and Mt-thyme oil hybrids (a), Na^+-Mt, thymol and Mt-thymol hybrids (b), Na^+-Mt, carvacrol and Mt-carvacrol hybrids (c) in the range of (a) 4000-500 cm^{-1} and Mt-thyme oil hybrids, Mt-thymol hybrids and Mt-carvacrol hybrids (d), in the range of (a) 4000–2500 cm^{-1}

4. 5. Simulation result

The simulation results (Figure 6) show - that the adsorption of thymol molecules onto Na^+-Mt nanoparticles took place in the external surface by creating hydrogen bonds between OH groups of thymol and OH groups of Na^+-Mt surface, and- that the adsorption was made through

the formation of hydrogen bonds between the thymol molecules, which explains the increase in the adsorption rate although there are a few OH groups in the external Na^+-Mt surface.

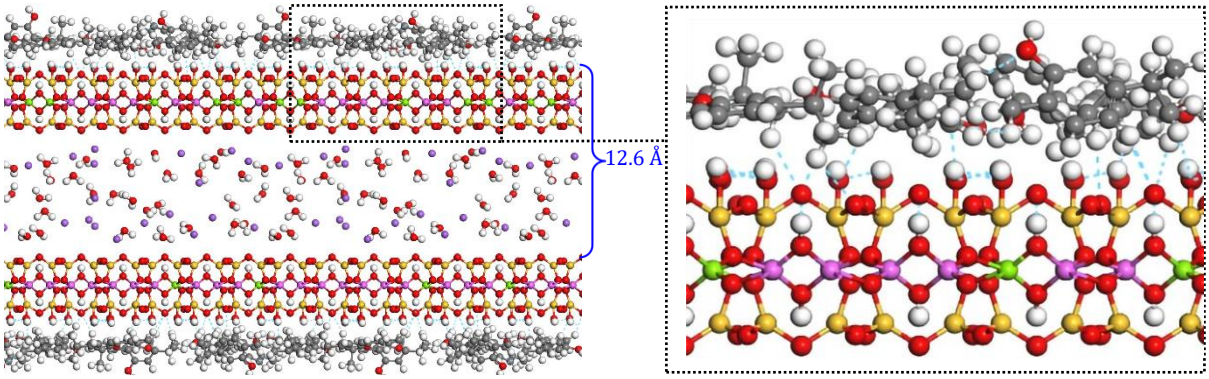

Fig. 6. (In left) Structure of modified Mt with EO molecules (side view), (In right) Zoom of part of EO OH groups bonded on surface OH groups of Na^+-Mt. Ball and stick colors: Dark purple (Na^+), gray (C), red (O), white (H), green (Mg), purple (Al), gold (Si).

This result was in correlation with the previous obtained experimental results such as - ATR-FTIR (strong electrostatic interactions on the Na^+-Mt surface), - XRD results where no increase of d-spacing was observed for all obtained Na^+-Mt hybrid materials (Figure 3) and - TG results also showing this kind of adsorption where it was observed that thyme EO, thymol, and carvacrol molecules released from Na^+-Mt surface above 180°C (Table 3) suggesting a strong bond.

4. 6. Release study

The qualitative release profiles of thyme oil, thymol and carvacrol from Na^+-Mt/thyme oil, Na^+-Mt/thymol, and Na^+-Mt/carvacrol hybrid materials were determined as follows: the Na^+-Mt nanoparticles loaded with EO, thymol or carvacrol was introduced in a vial of HPLC and was closed and placed at 25°C. The release was monitored every 24 hours using gas chromatography. The results of release in gas phase of thyme oil, thymol and carvacrol from the Na^+-Mt are illustrated in Figure 7, as well as the chromatograms of pure EO, thymol and carvacrol are presented.

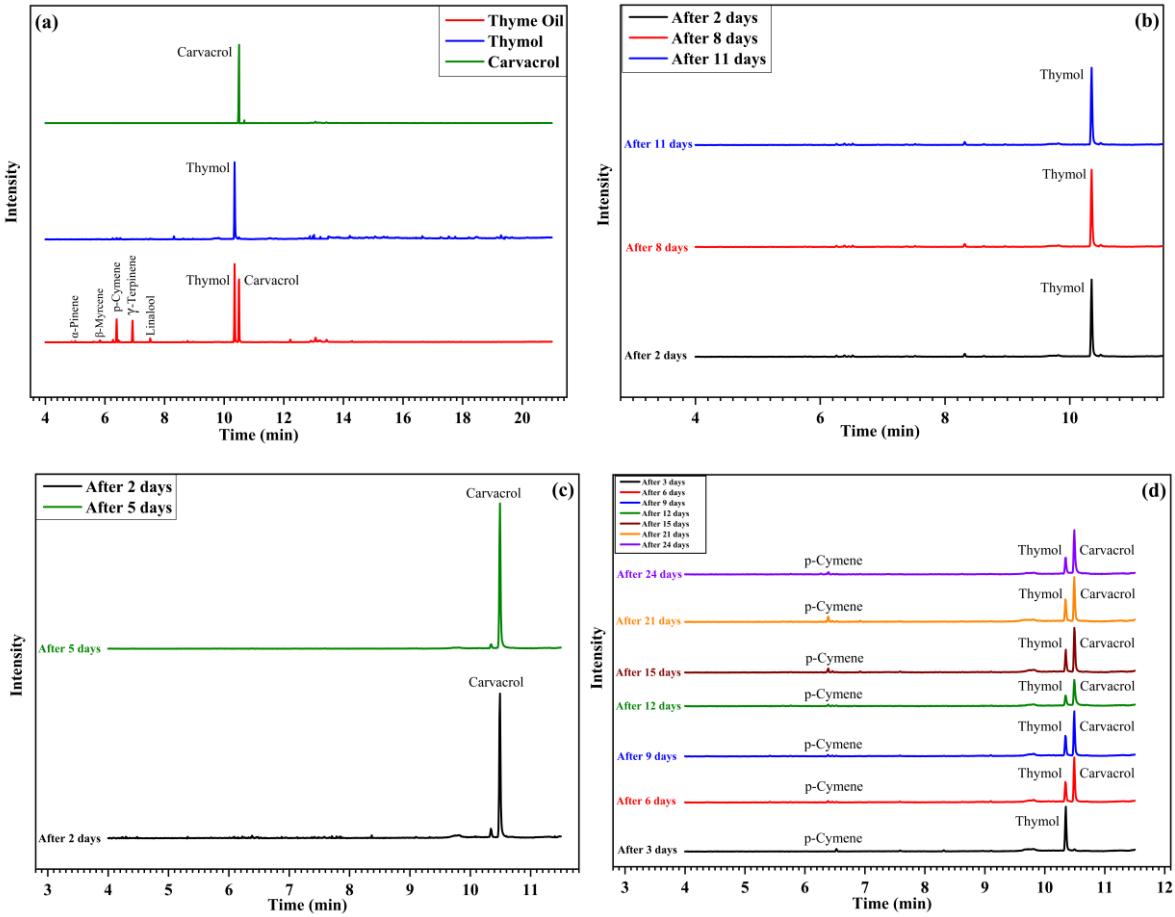

Fig. 7. Chromatograms of pure EO of thyme, thymol and carvacrol (a), and the qualitative release chromatograms of thymol (b), carvacrol (c), and thyme EO (d) from Na^{+}-Mt/OE hybrid materials

To better follow the release kinetics by gas chromatography, the constituents of the different adsorbents, thyme EO, thymol and carvacrol have been identified. Analysis of the chromatogram of thyme EO, thymol and carvacrol (Figure 7a) shows that the EO of thyme is essentially composed of seven different constituents with different percentages: thymol (39.22%), carvacrol (36.12%), p-cymene (11.06%), γ-terpinene (10.47%), linalool (1.8%), β-myrcene (0.82%) and α-pinene (0.52%). The vast majority of the composition of thyme oil are thymol and carvacrol. Chromatography analyzes show that the EO of thyme, thymol and carvacrol used are pure.

Chromatography analyzes of the release of thymol (Figure 7b) and carvacrol (Figure 7c), from their respective hybrid materials show that the EO constituents, thymol and carvacrol, remain stable in hybrid systems and show that adsorption of EO components like thymol and

carvacrol onto an inorganic porous material such as Na^+-Mt provide controlled release and protection against environmental conditions.

For release of thyme EO, the results show that there is a chemical selectivity on the release of the components of thyme oil from the hybrid materials Na^+-Mt/thyme, as shown in Figure7d; after the first three days of release, only two components are released, p-Cymene and thymol, the latter is released quantitatively compared to p-Cymene. After three days of release, the chromatograms obtained show that in addition to p-Cymene and thymol there is the release of carvacrol with a significant amount. The ratio of carvacrol and thymol released is raised by increasing release of carvacrol and decreasing of thymol. In addition, the extended release of all EO and the chemical stability are remarked. These results make it possible to know the selectivity of the kinetic release of the active compound of the EO.

5. Conclusion

The thyme EO, and its constituents such as thymol and carvacrol were adsorbed on Na^+-Mt according an evaporation/adsorption process without using organic solvents and without using a high temperature. The original adsorption procedure for EO retention on clay surface proposed in this study presents some advantages reported in the following notes:

1. It avoids the use of organic solvents, unwanted in various functional applications (due to their toxicity degree).
2. It avoids the heating of EO and volatile molecules such as thymol and carvacrol, so as not to endanger their physical-chemical properties.
3. It leads to prepare Na^+-Mt loaded with EO like thyme oil and/or volatile molecules such as thymol and carvacrol in the powder form (powder hybrid nanomaterials), which is desirable and more applicable for various functional applications.

In summary, the combined simulation results and all obtained experimental results, confirm that, the adsorption process of thyme EO, thymol, and carvacrol molecules on the Na^+-Mt took place on the external surface of the clay mineral by hydrogen bonds between EO, thymol or carvacrol OH groups and OH groups of Na^+-Mt surface, and by hydrogen bonds between adsorbed molecules.

The release study by chromatographic in gas phase shows that the adsorption of EO like thyme oil and its volatile constituents such as thymol and carvacrol onto an inorganic porous material such as Na^+-Mt provide extended controlled release of all adsorbed volatile molecules

and their chemical stability due to the protection against environmental conditions. In addition, a selectivity of the kinetic release in gas phase of constituent thyme oil such as the carvacrol and thymol from the powder of Na^+-Mt has been observed.

Acknowledgments

The authors are sincerely thankful to *MESRSFC, CNRST-Morocco* and *UMP* for financial support of *Project PPR 15–17* and *PARA1-2019*. The authors are thankful to the *Dr Faiza BERGAYA* from CNRS *Laboratory* Orleans for valuable corrections and suggestions to improve the content of the manuscript.

References

[1] *Y.X. Seow, C.R. Yeo, H.L. Chung, H.G. Yuk, Plant Essential Oils as Active Antimicrobial Agents, Crit. Rev. Food Sci. Nutr. 54 (2014) 625–644. https://doi.org/10.1080/10408398.2011.599504.*

[2] *M. Hernández-López, Z.N. Correa-Pacheco, S. Bautista-Baños, L. Zavaleta-Avejar, J.J. Benítez-Jiménez, M.A. Sabino-Gutiérrez, P. Ortega-Gudiño, Bio-based composite fibers from pine essential oil and PLA/PBAT polymer blend. Morphological, physicochemical, thermal and mechanical characterization, Mater. Chem. Phys. 234 (2019) 345–353. https://doi.org/10.1016/j.matchemphys.2019.01.034.*

[3] *A. El Asbahani, K. Miladi, W. Badri, M. Sala, E.H.A. Addi, H. Casabianca, A. El Mousadik, D. Hartmann, A. Jilale, F.N.R. Renaud, A. Elaissari, Essential oils: From extraction to encapsulation, Int. J. Pharm. 483 (2015) 220–243. https://doi.org/10.1016/j.ijpharm.2014.12.069.*

[4] *Maes, C., Bouquillon, S., Fauconnier, M.L., Encapsulation of Essential Oils for the Development of Biosourced Pesticides with Controlled Release: A Review, Molecules. 24 (2019) 2539. https://doi.org/10.3390/molecules24142539.*

[5] *J.R. Calo, P.G. Crandall, C.A. O'Bryan, S.C. Ricke, Essential oils as antimicrobials in food systems - A review, Food Control. 54 (2015) 111–119. https://doi.org/10.1016/j.foodcont.2014.12.040.*

[6] *E.W. Abd El-Wahab, T.E., Ebadah, I.M.A. and Zidan, Control of Varroa Mite by Essential Oils and Formic Acid with Their Effects on Grooming Behaviour of Honey Bee Colonies, J. Basic Appl. Sci. Res. 2 (2015) 7674–7680.*

[7] *F.A. Al-Bayati, Synergistic antibacterial activity between Thymus vulgaris and Pimpinella anisum essential oils and methanol extracts, J. Ethnopharmacol. 116 (2008) 403–406. https://doi.org/10.1016/j.jep.2007.12.003.*

[8] *R. Pavela, G. Benelli, Essential Oils as Ecofriendly Biopesticides? Challenges and Constraints, Trends Plant Sci. 21 (2016) 1000–1007. https://doi.org/10.1016/j.tplants.2016.10.005.*

[9] *M. Perricone, E. Arace, M.R. Corbo, M. Sinigaglia, A. Bevilacqua, Bioactivity of essential oils: A review on their interaction with food components, Front. Microbiol. 6*

(2015) 1–7. https://doi.org/10.3389/fmicb.2015.00076.

[10] H. Ramzi, M.R. Ismaili, M. Aberchane, S. Zaanoun, Chemical characterization and acaricidal activity of Thymus satureioides C. & B. and Origanum elongatum E. & M. (Lamiaceae) essential oils against Varroa destructor Anderson & Trueman (Acari: Varroidae), Ind. Crops Prod. 108 (2017) 201–207. https://doi.org/10.1016/j.indcrop.2017.06.031.

[11] M. Fennane, M. Rejdali, Aromatic and medicinal plants of Morocco : Richness , diversity and threats Plantes aromatiques et médicinales du Maroc : Richesse , diversité et menaces, (2016).

[12] O. Borugă, C. Jianu, C. Mişcă, I. Goleţ, A.T. Gruia, F.G. Horhat, Thymus vulgaris essential oil: chemical composition and antimicrobial activity, J. Med. Life. 7 . 3 (2014) 56–60.

[13] S. Gaysinsky, P.M. Davidson, B.D. Bruce, J. Weiss, Growth inhibition of Escherichia coli O157:H7 and Listeria monocytogenes by carvacrol and eugenol encapsulated in surfactant micelles, J. Food Prot. 68 (2005) 2559–2566. https://doi.org/10.4315/0362-028X-68.12.2559.

[14] Á. Perdones, A. Chiralt, M. Vargas, Properties of film-forming dispersions and films based on chitosan containing basil or thyme essential oil, Food Hydrocoll. 57 (2016) 271–279. https://doi.org/10.1016/j.foodhyd.2016.02.006.

[15] Q. Sabahi, H. Gashout, P.G. Kelly, E. Guzman-Novoa, Continuous release of oregano oil effectively and safely controls Varroa destructor infestations in honey bee colonies in a northern climate, Exp. Appl. Acarol. 72 (2017) 263–275. https://doi.org/10.1007/s10493-017-0157-3.

[16] B. Kouache, M. Brada, A. Saadi, M.L. Fauconnier, G. Lognay, S. Heuskin, Chemical composition and acaricidal activity of Thymus algeriensis essential oil against Varroa destructor, Nat. Prod. Commun. 12 (2017) 135–138. https://doi.org/10.1177/1934578x1701200138.

[17] K. Can Baser, Biological and Pharmacological Activities of Carvacrol and Carvacrol Bearing Essential Oils, Curr. Pharm. Des. 14 (2008) 3106–3119. https://doi.org/10.2174/138161208786404227.

[18] *M.D. Ellis, F.P. Baxendale, Toxicity of Seven Monoterpenoids to Tracheal Mites (Acari: Tarsonemidae) and Their Honey Bee (Hymenoptera: Apidae) Hosts When Applied as Fumigants, J. Econ. Entomol. 90 (1997) 1087–1091. https://doi.org/10.1093/jee/90.5.1087.*

[19] *C. Moiteiro, T. Esteves, L. Ramalho, R. Rojas, S. Alvarez, S. Zacchino, H. Bragança, Essential oil characterization of two Azorean Cryptomeria japonica populations and their biological evaluations, Nat. Prod. Commun. 8 (2013) 1785–1790. https://doi.org/10.1177/1934578x1300801233.*

[20] *G. Glavan, S. Novak, J. Božič, A. Jemec Kokalj, Comparison of sublethal effects of natural acaricides carvacrol and thymol on honeybees, Pestic. Biochem. Physiol. (2020). https://doi.org/10.1016/j.pestbp.2020.104567.*

[21] *N. Petchwattana, P. Naknaen, Utilization of thymol as an antimicrobial agent for biodegradable poly(butylene succinate), Mater. Chem. Phys. 163 (2015) 369–375. https://doi.org/10.1016/j.matchemphys.2015.07.052.*

[22] *B. Salehi, A.P. Mishra, I. Shukla, M. Sharifi-Rad, M. del M. Contreras, A. Segura-Carretero, H. Fathi, N.N. Nasrabadi, F. Kobarfard, J. Sharifi-Rad, Thymol, thyme, and other plant sources: Health and potential uses, Phyther. Res. 32 (2018) 1688–1706. https://doi.org/10.1002/ptr.6109.*

[23] *R.K. Lima, M. das G. Cardoso, J.C. Moraes, S.M. Carvalho, V.G. Rodrigues, L.G.L. Guimarães, Chemical composition and fumigant effect of essentialoil of Lippia sidoides Cham. and monoterpenes against Tenebrio molitor (L.) (coleoptera: tenebrionidae), Ciência e Agrotecnologia. 35 (2011) 664–671. https://doi.org/10.1590/s1413-70542011000400004.*

[24] *M.B. Isman, S. Miresmailli, C. MacHial, Commercial opportunities for pesticides based on plant essential oils in agriculture, industry and consumer products, Phytochem. Rev. 10 (2011) 197–204. https://doi.org/10.1007/s11101-010-9170-4.*

[25] *Y. Zhang, Y. Niu, Y. Luo, M. Ge, T. Yang, L. Yu, Q. Wang, Fabrication, characterization and antimicrobial activities of thymolloaded zein nanoparticles stabilized by sodium caseinate-chitosan hydrochloride double layers, Food Chem. 142 (2014) 269–275. https://doi.org/10.1016/j.foodchem.2013.07.058.*

[26] *A. Giannakas, I. Tsagkalias, D.S. Achilias, A. Ladavos, A novel method for the preparation of inorganic and organo-modified montmorillonite essential oil hybrids, Appl. Clay Sci. 146 (2017) 362–370. https://doi.org/10.1016/j.clay.2017.06.018.*

[27] *M. El Miz, S. Salhi, I. Chraibi, A. El Bachiri, M.-L. Fauconnier, A. Tahani, Characterization and Adsorption Study of Thymol on Pillared Bentonite, Open J. Phys. Chem. 04 (2014) 98–116. https://doi.org/10.4236/ojpc.2014.43013.*

[28] *El Miz, M., Salhi, S., El Bachiri, A., Wathelet, J. P., Tahani, A., Adsorption of essential oil components of Lavandula Angustifolia on Pillared modified bentonite, Int. J. Adv. Sci. Tech. Res. 4 (2014) 349–373.*

[29] *El Miz, M., Salhi, S., El Bachiri, A., Wathelet, J. P., Tahani, A., Adsorption of essential oil components of Lavandula angustifolia on sodium modified bentonite from Nador (North-East Morocco), African J. Biotechnol. 13 (2014) 3413–3425. https://doi.org/10.5897/AJB2013.13450.*

[30] *M.A. Kinninmonth, C.M. Liauw, J. Verran, R. Taylor, V. Edwards-Jones, D. Shaw, M. Webb, Investigation into the suitability of layered silicates as adsorption media for essential oils using FTIR and GC-MS, Appl. Clay Sci. 83–84 (2013) 415–425. https://doi.org/10.1016/j.clay.2013.07.009.*

[31] *M.M.G. Nguemtchouin, M.B. Ngassoum, L.S.T. Ngamo, X. Gaudu, M. Cretin, Insecticidal formulation based on Xylopia aethiopica essential oil and kaolinite clay for maize protection, Crop Prot. 29 (2010) 985–991. https://doi.org/10.1016/j.cropro.2010.06.007.*

[32] *M.M.G. Nguemtchouin, M.B. Ngassoum, L.S.T. Ngamo, P.M. Mapongmetsem, J. Sieliechi, F. Malaisse, G.C. Lognay, E. Haubruge, T. Hance, Adsorption of essential oil components of Xylopia aethiopica (Annonaceae) by kaolin from Wak, Adamawa province (Cameroon), Appl. Clay Sci. 44 (2009) 1–6. https://doi.org/10.1016/j.clay.2008.10.010.*

[33] *M.G.M. Nguemtchouin, M.B. Ngassoum, P. Chalier, R. Kamga, L.S.T. Ngamo, M. Cretin, Ocimum gratissimum essential oil and modified montmorillonite clay, a means of controlling insect pests in stored products, J. Stored Prod. Res. 52 (2013) 57–62. https://doi.org/10.1016/j.jspr.2012.09.006.*

[34] *J.J. Hwang, T.W. Ma, Preparation, morphology, and antibacterial properties of polyacrylonitrile/montmorillonite/silver nanocomposites, Mater. Chem. Phys. 136 (2012) 613–623. https://doi.org/10.1016/j.matchemphys.2012.07.034.*

[35] *S.M. El-Kousy, H.G. El-Shorbagy, M.A.A. El-Ghaffar, Chitosan/montmorillonite composites for fast removal of methylene blue from aqueous solutions, Mater. Chem. Phys. 254 (2020) 123236. https://doi.org/10.1016/j.matchemphys.2020.123236.*

[36] *T.J. Gutiérrez, A.G. Ponce, V.A. Alvarez, Nano-clays from natural and modified montmorillonite with and without added blueberry extract for active and intelligent food nanopackaging materials, Mater. Chem. Phys. 194 (2017) 283–292. https://doi.org/10.1016/j.matchemphys.2017.03.052.*

[37] *A. Bernardos, M. Bozik, S. Alvarez, M. Saskova, E. Perez-Esteve, P. Kloucek, M. Lhotka, A. Frankova, R. Martinez-Manez, The efficacy of essential oil components loaded into montmorillonite against Aspergillus niger and Staphylococcus aureus, Flavour Fragr. J. 34 (2019) 151–162. https://doi.org/10.1002/ffj.3488.*

[38] *M. El Miz, H. Akichoh, D. Berraaouan, S. Salhi, A. Tahani, Chemical and Physical Characterization of Moroccan Bentonite Taken from Nador (North of Morocco), Am. J. Chem. 2017 (2017) 105–112. https://doi.org/10.5923/j.chemistry.20170704.01.*

[39] *H. Zaitan, D. Bianchi, O. Achak, T. Chafik, A comparative study of the adsorption and desorption of o-xylene onto bentonite clay and alumina, J. Hazard. Mater. 153 (2008) 852–859. https://doi.org/10.1016/j.jhazmat.2007.09.070.*

[40] *L. Ammann, F. Bergaya, G. Lagaly, Determination of the cation exchange capacity of clays with copper complexes revisited, Clay Miner. 40 (2005) 441–453. https://doi.org/10.1180/0009855054040182.*

[41] *F. Bergaya, M. Vayer, CEC of clays: Measurement by adsorption of a copper ethylenediamine complex, Appl. Clay Sci. 12 (1997) 275–280. https://doi.org/10.1016/S0169-1317(97)00012-4.*

[42] *F. Bergaya, B.K.G. Theng, G. Lagaly, Handbook of Clay Science, (Eds.), 2006. http://books.google.com/books?id=uVbam9Snw5sC&pgis=1.*

[43] *C. Tournassat., C.I. Steefel., I.C. Bourg., F. Bergaya., Natural and Engineered Clay Barriers, (Eds.), 2015.*

[44] *H. Schulz, R. Quilitzsch, H. Krüger, Rapid evaluation and quantitative analysis of thyme, origano and chamomile essential oils by ATR-IR and NIR spectroscopy, J. Mol. Struct. 661–662 (2003) 299–306. https://doi.org/10.1016/S0022-2860(03)00517-9.*

[45] *L.M. Wu, D.S. Tong, L.Z. Zhao, W.H. Yu, C.H. Zhou, H. Wang, Fourier transform infrared spectroscopy analysis for hydrothermal transformation of microcrystalline cellulose on montmorillonite, Appl. Clay Sci. 95 (2014) 74–82. https://doi.org/10.1016/j.clay.2014.03.014.*

[46] *M. El Miz, K. Essifi, S. Salhi, F. Bergaya, A. Tahani, Synthesis and Characterization of CPC Organo-modified and Al 13 Pillared Modified Bentonite ., Mor. J. Chem. 2 (2019) 242–253.*

[47] *P. Djomgoue, D. Njopwouo, FT-IR Spectroscopy Applied for Surface Clays Characterization, J. Surf. Eng. Mater. Adv. Technol. 03 (2013) 275–282. https://doi.org/10.4236/jsemat.2013.34037.*

[48] *S.M.L. Silva, C.R.C. Braga, M.V.L. Fook, C.M.O. Raposo, L.H. Carvalho, E.L. Canedo, Application of Infrared Spectroscopy to Analysis of Chitosan/Clay Nanocomposites, Infrared Spectrosc. - Mater. Sci. Eng. Technol. (2012). https://doi.org/10.5772/35522.*